Journal of Materials Chemistry B

PAPER

View Article Online
View Journal | View Issue

Published on 23 June 2015. Downloaded by Xiamen University on 8/17/2018 7:09:25 AM.

Cite this: J. Mater. Chem. B, 2015, 3, 6255

Two-dimensional antibacterial Pd@Ag nanosheets with a synergetic effect of plasmonic heating and Ag^+ release†

Shiguang Mo,[a] Xiaolan Chen,*[a] Mei Chen,[a] Caiyun He,[b] Yinghua Lu[b] and Nanfeng Zheng*[a]

Received 5th May 2015,
Accepted 22nd June 2015

DOI: 10.1039/c5tb00830a

www.rsc.org/MaterialsB

In this work, a novel bactericidal agent based on two-dimensional Pd@Ag nanosheets (Pd@Ag NSs) that is responsive to near-infrared (NIR) light has been developed. These Pd@Ag NSs were prepared by reducing silver ions on the surface of Pd nanosheets (Pd NSs) seeds by formaldehyde, and displayed excellent NIR absorption and photothermal conversion properties. In addition, the NIR irradiation triggers the release of more Ag^+ from the Pd@Ag NSs. Upon exposure to a NIR laser at a low power density (0.5 W cm^{-2}), Pd@Ag NSs kill both Gram-negative (*Escherichia coli*, *E. coli*) and Gram-positive (*Staphylococcus aureus*, *S. aureus*) bacteria effectively by the synergistic effect of plasmonic heating and Ag^+ release, which is much higher than either plasmonic heating or Ag^+ alone. Such a novel nanomaterial is promising as an adjuvant therapeutic method for the treatment of patients suffering from severe bacterial infections.

1 Introduction

Antibiotics, which have served human beings for decades and saved millions of lives, are widely used to treat diseases caused by bacterial pathogens.[1] However, the general overuse of antibiotics has led to the emergence of antibiotic-resistant bacterial strains,[2] which have become a pressing threat to public health.[3] Therefore, it is highly desirable to develop novel antibacterial materials and/or new methods for effective killing of these pathogenic bacteria.[4–12]

Recently, photothermal therapy (PTT) has been proposed as a promising approach for killing bacteria.[10,13–22] In the technique, photoabsorbing agents are delivered to target bacteria and irradiated with an appropriate light. The absorbed optical energy is then converted into heat, which results in irreparable physical damage and subsequent bacterial death. In general, near-infrared (NIR, 700–1100 nm) light is preferred for such an application owing to its capability for deeper penetration into biological tissues.[20] To date, several types of NIR-absorbing nanomaterials, including gold-based nanostructures,[21,22] carbon-based nanomaterials[13,19,20] (*e.g.* carbon nanotubes and graphene), silver hybrid nanoparticles[16,17] as well as silica-coated polypyrrole nanoparticles[18] have been developed for the treatment of pathogenic bacteria upon NIR laser irradiation. It was also reported that NIR irradiation triggered the release of Ag^+ ions from some Ag-containing nanostructures such as polymer–silver hybrid core–shell nanoparticles[17] and Au@Ag nanorods,[21] which provides a synergetic antibacterial effect by plasmonic heating and silver release.

Two-dimensional palladium nanosheets (Pd NSs) have recently attracted increasing attention in biomedical applications due to their fascinating physical and chemical properties, such as well-defined thicknesses, sizes and tunable surface plasmon resonance (SPR) peaks in the NIR region, high photothermal conversion efficiency, excellent photothermal stability and biocompatibility.[23,24] Our group has successfully used them as NIR absorbing agents for the photothermal treatment of cancer both *in vitro* and *in vivo*.[23–28] Moreover, by the epitaxial growth method, bimetal Pd@Ag or Pd@Au nanosheets with well-defined sizes and morphology can be facilely prepared, providing us with great opportunities to explore their biological application.[29–31]

Herein, we demonstrate for the first time that Pd@Ag nanosheets (Pd@Ag NSs) can be used as an efficient antibacterial agent for killing pathogenic bacteria. Pd@Ag NSs with a surface plasmon resonance peak at ~830 nm in the NIR region can be easily prepared by reducing silver ion on the surface of Pd

[a] State Key Laboratory for Physical Chemistry of Solid Surfaces, Collaborative Innovation Center of Chemistry for Energy Materials, Engineering Research Center for Nano-Preparation Technology of Fujian Province, and Department of Chemistry, College of Chemistry and Chemical Engineering, Xiamen University, Xiamen 361005, China. E-mail: chenxl@xmu.edu.cn, nfzheng@xmu.edu.cn
[b] Department of Chemical and Biochemical Engineering, College of Chemistry and Chemical Engineering, Xiamen University, Xiamen 361005, China

† Electronic supplementary information (ESI) available: Dispersion stability of Pd@Ag NSs in different solutions, TEM images of Pd@Ag NSs and Ag nanoprisms before and after the laser irradiation, silver released from Pd@Ag NSs with and without light irradiation under a N_2 atmosphere, infrared thermal imaging of Pd@Ag NSs-treated bacteria, images of bacteria colonies and histogram of bacterial viability with different treatments. See DOI: 10.1039/c5tb00830a

Published on 23 June 2015. Downloaded by Xiamen University on 8/17/2018 7:09:25 AM.

nanosheets (Pd NSs) seeds by formaldehyde, and can kill bacteria through photothermal lysis. Moreover, NIR irradiation triggers the release of more Ag^+ from the Pd@Ag NSs, creating an enhanced antibacterial ability. In the presence of NIR irradiation at a low power density (0.5 W cm^{-2}), both Gram-negative and Gram-positive bacteria can be effectively killed by Pd@Ag NSs due to the synergistic antibacterial effect of plasmonic heating and Ag^+ release, which could not be simply achieved by either plasmonic heating or Ag^+ alone.

2 Experimental section

Materials

$Pd(acac)_2$ and $AgNO_3$ were purchased from Alfa Aesar. Poly(vinylpyrrolidone) (PVP, M_W = 30 000), *N*,*N*-dimethylformamide (DMF), methanal (HCHO) solution (40%), and tetrabutylammonium bromide (TBAB) were purchased from Sinopharm Chemical Reagent Co. Ltd (China). Propidium iodide (PI) was ordered from Sigma-Aldrich. HeLa cells were obtained from the cell storeroom of Chinese Academy of Sciences. All of the reagents were used as received without further purification.

Synthesis of Pd nanosheets (Pd NSs)

Pd NSs were synthesized according to the previously reported procedure.[23] In brief, 50.0 mg of $Pd(acac)_2$, 160.0 mg of PVP and 160 mg of TBAB were mixed together with 10 mL of DMF and 2 mL of water. The obtained yellow solution was transferred to a glass pressure vessel. The vessel was then charged with CO to 1 bar and heated at 60 °C for 2.5 h before naturally cooling to room temperature.

Synthesis of Pd@Ag nanosheets (Pd@Ag NSs)

0.2 mL of the above synthesized Pd NSs solution was mixed with the appropriate amount of $AgNO_3$ solution (0.025 mol L^{-1}), followed by adding 0.9 mL of HCHO solution (40%). The mixture was stirred for 10 min to obtain a homogeneous solution, and left undisturbed at room temperature overnight. The obtained Pd@Ag NSs were washed three times by acetone and ethanol to remove the unreacted silver ions and stored at 4 °C for future use.

Measurement of photothermal effect

To examine the photothermal effect induced by the NIR irradiation, 1.5 mL of 15 μg mL^{-1} Pd NSs and 7.1 μg mL^{-1} Pd@Ag NSs solutions were irradiated for 10 min by a NIR laser (808 nm, 0.5 W cm^{-2}), respectively. The temperature changes of the solutions were monitored using a submerged thermocouple microprobe.

Ag^+ release from Pd@Ag NSs

The Pd@Ag NSs suspensions placed in a 96-well plate were subjected to NIR laser irradiation (0.5 W cm^{-2}) for 10 min. The irradiated solutions were then collected and centrifuged to obtain the supernatant. Other Pd@Ag NSs suspensions without NIR laser irradiation were used as the negative control. The released Ag^+ concentration was determined by ICP-MS (7500CE, Agilent).

Bacterial cultivation

Before each experiment, all samples and glassware were sterilized by autoclaving at 121 °C for 30 min. The Luria–Bertani (LB) medium was prepared by mixing 10 g of tryptone, 5 g of yeast extract, and 10 g of NaCl in 1000 mL of deionized water. *S. aureus* and *E. coli* strains were cultured in LB nutrient broth at 37 °C overnight. The bacteria were diluted to 10^7 CFU mL^{-1} by PBS, then incubated with Pd@Ag NSs in 96-well plates for 30 min before NIR laser irradiation.

Photothermal killing of bacteria

For photothermal treatment of bacteria, diluted *S. aureus* and *E. coli* in 96-well plates were vortexed for 30 min with 9.5 μg mL^{-1} and 5.9 μg mL^{-1} of Pd@Ag NSs in which the Ag concentrations reached to 8 and 5 μg mL^{-1}, respectively. Then photothermal therapy was carried out for 10 min by using a continuous wavelength laser (0.5 W cm^{-2} operating at 808 nm) as an excitation light source. After irradiation, the bacteria (30 μL) were transferred to tryptic agar plates and incubated for 24 h at 37 °C and pictures were taken using a camera. The numbers of surviving colonies for each plate were counted by diluting to appropriate concentration and incubation for 48 h at 37 °C. The bacteria with or without exposure to 808 nm light were also stained by PI and photos were taken using a confocal fluorescence microscope.

The cytotoxicity of Pd and Pd@Ag NSs to HeLa cells

Different concentrations of Pd and Pd@Ag NSs were incubated with HeLa cells for 24 h, respectively. A stock solution of MTT (25 μL, 5 mg mL^{-1}) was added into each well. After 4 h incubation at 37 °C, the MTT solution was replaced with 150 μL DMSO in each well. The plates were gently shaken for 10 min at room temperature before measuring the absorbance at 490 nm using a microplate reader.

Characterization

The transmission electron microscope (TEM) images were obtained using a JEOL 1400 TEM at 100 kV. UV-Vis-NIR absorption spectra were obtained using a Cary 5000 scan UV-Vis-NIR spectrophotometer.

3 Results and discussion

Synthesis and characterization of Pd@Ag NSs

Scheme 1 illustrates our Pd@Ag NSs-based strategy for killing bacteria by the synergetic effect of plasmonic heating and Ag^+ release. After incubating Pd@Ag NSs with bacteria, the Pd@Ag NSs can attach to the surface of bacteria. Under irradiation with an NIR laser, both the heat produced from the photothermal transducing capacity of Pd@Ag NSs and Ag^+ release triggered by illumination can effectively kill the bacteria.

The Pd@Ag NSs were synthesized by reduction of $AgNO_3$ with formaldehyde on the surface of Pd nanosheets (Pd NSs) according to our previously reported procedure with slight modification.[29] As shown in Fig. 1b, the prepared Pd@Ag NSs have hexagonal plate-like shapes with an average diameter of about 85 nm, which are similar to that of the original Pd NSs

 This journal is © The Royal Society of Chemistry 2015

Published on 23 June 2015. Downloaded by Xiamen University on 8/17/2018 7:09:25 AM.

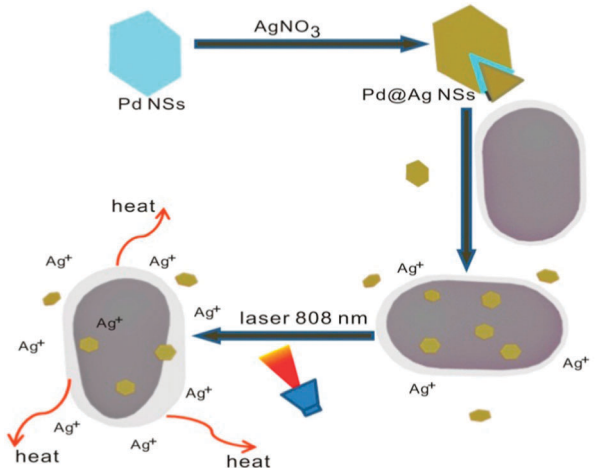

Scheme 1 Schematic illustration of the Pd@Ag NSs for synergetic treatment of bacteria. "Ag^{+}" stands for silver ions released from Pd@Ag NSs.

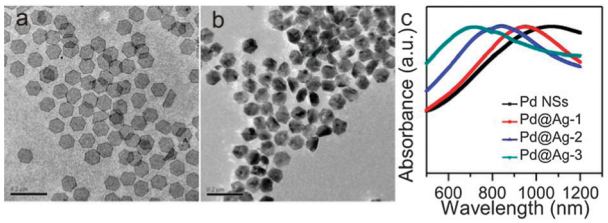

Fig. 1 TEM images of Pd NSs (a), Pd@Ag NSs (b) and UV-Vis-NIR absorption spectra of parental Pd NSs and different Pd@Ag NSs with the feeding Ag/Pd molar ratios of 4.5 (Pd@Ag-1, 950 nm), 6.3 (Pd@Ag-2, 830 nm) and 8.2 (Pd@Ag-3, 710 nm). The scale bar = 0.2 μm.

seeds (Fig. 1a). By careful adjusting the feeding amount of $AgNO_3$, a series of Pd@Ag NSs with different surface-plasmon-resonance (SPR) absorption peaks were obtained (Fig. 1c). As shown in Fig. 1c, the maximum optical absorptions were gradually blue-shifted as the Ag/Pd ratio increased. While the SPR peak of the parental Pd NSs was centered at ~1050 nm, the absorption peaks of the Pd@Ag nanosheets prepared with the Ag/Pd molar ratios of 4.5, 6.3 and 8.2 were shifted to ~950, 830, and 710 nm, respectively. Considering that the NIR laser (808 nm) will be used for our photothermal studies, Pd@Ag NSs with ~830 nm SPR peak were used in the following experiments.

The Pd@Ag NSs demonstrated good dispersity in water, PBS and cell medium containing 10% fetal bovine serum (FBS) (Fig. S1, ESI†), respectively. As shown in Fig. S1 (ESI†), the mean hydrodynamic diameters for Pd@Ag NSs dispersed in water, PBS and cell medium remained almost unchanged over three days. In addition, when the NSs stored in these solutions for three days (Fig. S2, ESI†), no significant decrease in absorption intensity has been observed. These results indicated that Pd@Ag NSs had good dispersion stability in physiological solutions.

Photothermal effects and NIR-triggered Ag^{+} release

The strong NIR absorption property and good dispersion stability of Pd@Ag NSs stimulated us to further explore their photothermal transfer capability. To perform this, both Pd@Ag NSs (7.1 μg mL^{-1}) and Pd NSs (15 μg mL^{-1}) solutions were exposed to the 808 nm laser at a power density of 0.5 W cm^{-2} for 10 min. As illustrated in Fig. 2a, upon the 10 min irradiation Pd@Ag NSs showed a temperature increase up to 19 °C. In comparison, the temperature elevation for the 15 μg mL^{-1} of Pd NSs, whose concentration was twice that of Pd@Ag NSs, was only 17 °C under the same irradiation conditions. Since the maximum absorption of Pd@Ag NSs at ~830 nm matches better with the 808 nm laser than that of Pd NSs with a wide absorption near 1100 nm, the laser energy of 808 nm can be more efficiently transformed to heat by Pd@Ag NSs than Pd NSs. It should be noted that water under the same irradiation conditions displayed a negligible change. In addition, compared to other two-dimensional (2D) pure Ag nanostructures, such as Ag nanoprisms,[32] the prepared Pd@Ag NSs display better photothermal stability (Fig. S3, ESI†). These data clearly demonstrated that the as-prepared Pd@Ag NSs had excellent photothermal capability and be expected to be a novel photothermal agent for inhibiting the cell growth of bacteria.

Considering that Ag^{+} itself has been well-documented as an efficient antibacterial agent, the silver release from the Pd@Ag NSs upon NIR irradiation was characterized by ICP-MS as well. As shown in Fig. 2b, the release amounts of silver from Pd@Ag NSs were highly dependent on whether the samples were subjected to NIR irradiation. At both concentrations of 5.9 and 9.5 ppm, the 10 min NIR irradiation of Pd@Ag NSs (0.5 W cm^{-2}, 808 nm) led to an increase in the amount of silver released from Pd@Ag NSs by 3–4 times, compared to non-irradiated controls.

It was reported that ion release from nanosilver (nAg) colloids was a cooperative oxidation process requiring both dissolved dioxygen and protons.[33] We infer that the release of silver from the Pd@Ag NSs might follow a similar mechanism. Under aerobic conditions, the zero-valent silver on the surface of Pd@Ag NSs can be oxidized to Ag(I), which reacts with protons in the weak acid medium to generate Ag^{+}. Besides, when illuminated with NIR, the Pd@Ag NSs converted the light to heat, giving rise to a rapid increase in the surface temperature of the metal, triggering the fast release of silver from the Pd@Ag NSs. We conducted a control experiment under a N_2 atmosphere. It was found that there was some silver released

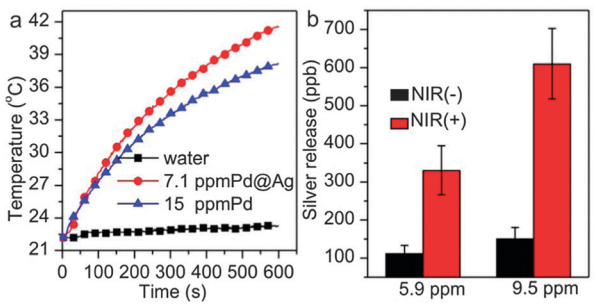

Fig. 2 (a) The temperature *versus* time plots were recorded for Pd and Pd@Ag NSs suspensions upon irradiation by a 0.5 W cm^{-2} 808 nm laser. (b) Silver released from 5.9 and 9.5 ppm of Pd@Ag NSs (containing 5 and 8 μg mL^{-1} Ag, respectively) with and without light irradiation (0.5 W cm^{-2} for 10 min).

Published on 23 June 2015. Downloaded by Xiamen University on 8/17/2018 7:09:25 AM.

(Fig. S4, ESI†), but it was lower than that in aerobic conditions with the same irradiation (Fig. 2b). The primary results indicated that the oxygen played an important role for both the oxidation of Ag(0) on the surface of Pd@Ag NSs and the silver released from the Pd@Ag NSs. Of course, more work would be needed to elucidate the detailed oxidation and release mechanism.

In vitro cytotoxicity study of Pd and Pd@Ag NSs

Before any nanomaterial is used for *in vivo* therapy, its potential toxicity to host cells is a concern. We first performed the standard MTT (methyl thiazolyl tetrazolium) assay to examine the cytotoxicity of both Pd and Pd@Ag NSs to HeLa cells. Different amounts of Pd and Pd@Ag NSs were added to wells containing HeLa cells. After incubation for 24 h, the cell viability was quantified by the MTT assay. As observed from Fig. 3b, Pd@Ag NSs exhibited higher cytotoxicity to HeLa cells compared to Pd NSs (Fig. 3a). However, when the concentration of Pd@Ag NSs was in the range of 0–12 μg mL^{-1} (containing $\leq$10 μg mL^{-1} Ag), the cells still had a more than 75% survival rate. All subsequent experiments were performed under these conditions unless indicated.

Antibacterial performances of Pd@Ag NSs

In our study, the Gram-negative bacteria of *Escherichia coli* (*E. coli*) and the Gram-positive bacteria of *Staphylococcus aureus* (*S. aureus*) were selected as the models to test the feasibility of using Pd@Ag NSs as a bactericidal agent. Both bacteria were first incubated with Pd@Ag NSs for 30 min, respectively. Then, the 808 nm NIR laser (0.5 W cm^{-2}) was utilized to irradiate the bacterial solutions for 10 min. It should be noted that since the wall thickness of *E. coli* is thinner than *S. aureus*,[34] the *E. coli* was more sensitive to treatments. In our experiments, 5.9 and 9.5 μg mL^{-1} of Pd@Ag NSs were used to treat *E. coli* and *S. aureus* respectively, resulting in the temperature increasing to 45 °C for *E. coli* (Fig. S5a, ESI†) and 50 °C for *S. aureus* (Fig. S5b, ESI†), respectively. Fig. 4 shows the TEM images of *E. coli* and *S. aureus* before and after incubation with Pd@Ag NSs with or without NIR irradiation. The *E. coli* and *S. aureus* bacteria alone have an integrated and smooth surface (Fig. 4a and d), whereas those bacteria incubated with Pd@Ag NSs were partially covered by Pd@Ag NSs (Fig. 4b and e). The NIR irradiation had a significant impact on the bacteria, and the cell walls of both bacteria were observed to be damaged apparently (Fig. 4c and f). After irradiation, in order to determine the bacterial viability, the treated bacteria were incubated on tryptic agar plates (Fig. 5a–h) and then diluted to an appropriate concentration to count the colonies of the bacteria (Fig. 5i and j). As shown in Fig. 5, the NIR laser alone did not kill bacteria effectively, and the viability of both *E. coli* and *S. aureus* was >93% (Fig. 5b, f, i(b) and j(f)). After incubation with Pd@Ag NSs without irradiation, the bacterial viability reached 71% for *E. coli* and 82% for *S. aureus*, respectively (Fig. 5c, g, i(c) and j(g)). Interestingly, when both bacteria were treated with Pd@Ag NSs

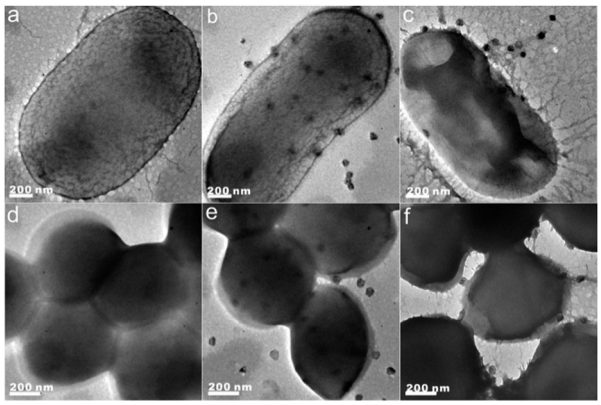

Fig. 4 TEM images of (a) *E. coli*, (b) *E. coli* incubated with Pd@Ag NSs, (c) *E. coli* incubated with Pd@Ag NSs under NIR irradiation, (d) *S. aureus*, (e) *S. aureus* incubated with Pd@Ag NSs, (f) *S. aureus* incubated with Pd@Ag NSs under NIR irradiation. Scale bars = 200 nm.

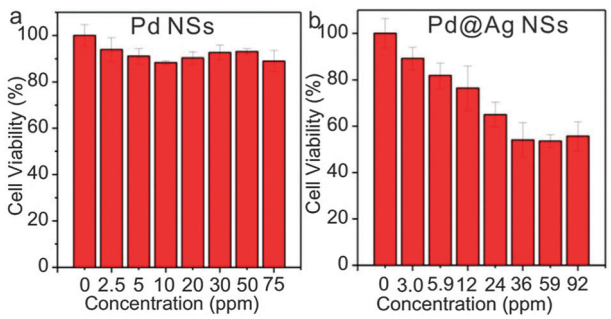

Fig. 3 The cytotoxicity of different concentrations of Pd NSs (a) and Pd@Ag NSs (b) to HeLa cells.

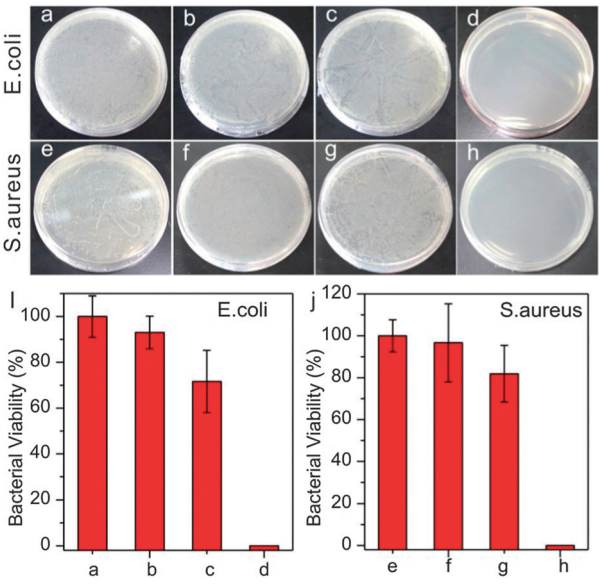

Fig. 5 Images of bacteria colonies and histograms of bacterial viability. (a) *E. coli*, (b) *E. coli* with NIR irradiation only, (c) *E. coli* treated with Pd@Ag NSs without NIR irradiation and (d) *E. coli* treated with Pd@Ag NSs with NIR irradiation. (e) *S. aureus*, (f) *S. aureus* with NIR irradiation only, (g) *S. aureus* treated with Pd@Ag NSs without NIR irradiation and (h) *S. aureus* treated with Pd@Ag NSs with NIR irradiation. Histograms of (i) *E. coli* and (j) *S. aureus* viability. The concentrations of Pd@Ag NSs are 5.9 μg mL^{-1} for *E. coli* and 9.5 μg mL^{-1} for *S. aureus*, respectively.

 This journal is © The Royal Society of Chemistry 2015

Published on 23 June 2015. Downloaded by Xiamen University on 8/17/2018 7:09:25 AM.

upon NIR light irradiation, a high antibacterial activity was observed. After 10 min of irradiation, almost 100% of bacteria were killed (Fig. 5d, h, i(d) and j(h)).

In order to further confirm the therapeutic effect of Pd@Ag NSs on *E. coli* and *S. aureus*, an activity assay based on the non-fluorescent dye propidium iodide (PI) was also carried out. PI can only enter through damaged bacteria membranes and be converted to a strongly red fluorescent dye through intercalating into DNA. Fluorescence images of *E. coli* and *S. aureus* incubated with Pd@Ag NSs with or without NIR irradiation are shown in Fig. 6. Without NIR irradiation, the bacteria were mostly alive (Fig. 6a and c). Extensive red fluorescence was observed after NIR irradiation (Fig. 6b and d), indicating that a large number of bacteria were killed. The maximal bacterial killing can be attributed to the two following aspects: plasmonic heating and silver release from Pd@Ag NSs under NIR irradiation. On the one hand, the Pd@Ag NSs can absorb the NIR light energy and transform it into heat, leading to irreversible bacteria membrane destruction (as demonstrated in Fig. 4c and f). On the other hand, the irradiation also induced more Ag^+ release from Pd@Ag NSs (Fig. 2b).

To illustrate the contribution of each factor to the death of bacteria, we performed the following experiments. First, the effects of heat on the bacterial viability were investigated by incubating *E. coli* at 45 °C and *S. aureus* at 50 °C, respectively. These temperatures were in accord with the temperature changes caused by laser irradiation (Fig. S5, ESI†). Within the same treatment time, the viability was reduced to 58% for *E. coli* and 61% for *S. aureus* respectively (Fig. S6, ESI†), indicating heat had an important impact on the bacterial viability. The bacteria-killing efficacies of Ag^+ released from Pd@Ag NSs were also investigated by first irradiating the Pd@Ag NSs for 10 min. After cooling to room temperature, the irradiated Pd@Ag NSs were then incubated with bacteria. As displayed in Fig. S2 (ESI†), the released Ag^+ decreases the viability of *E. coli* and *S. aureus* to 42.0% and 56% respectively.

Under NIR irradiation, Pd@Ag NSs killed bacteria more effectively than the photothermal effect or released Ag^+ alone, suggesting a significant synergic effect in the antibacterial activity in Pd@Ag NSs. According to the literature,[35] Ag^+ can be more toxic to bacteria and human cells compared to Ag NPs. After irradiation with NIR, the permeability of the bacteria wall changed, allowing the released Ag^+ to enter the bacteria and kill them more effectively. In addition, compared with *S. aureus*, *E. coli* was killed more by the NIR induced Ag^+ release possibly due to its smaller wall thickness. Overall, incubating Gram-negative and Gram-positive bacteria with Pd@Ag NSs followed by NIR irradiation provided the best therapeutic response due to both the plasmonic heating and Ag^+ release triggered by NIR irradiation.

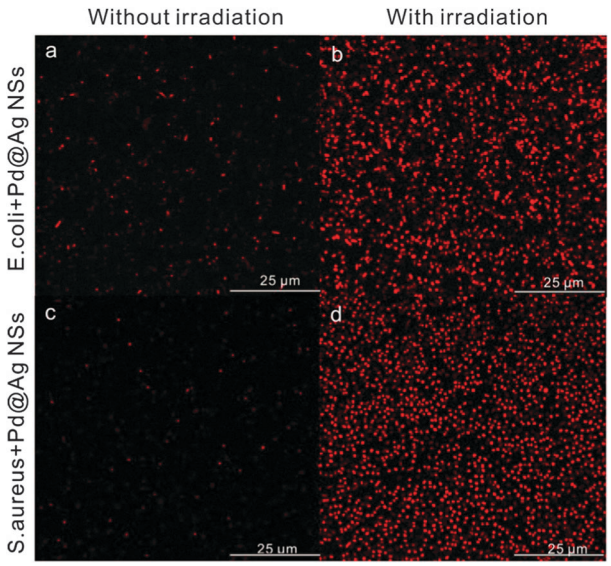

Fig. 6 Confocal fluorescence images of *E. coli* (a and b) and *S. aureus* (c and d) before (a and c) and after irradiation with NIR laser for 10 min (b and d).

4 Conclusion

In summary, we demonstrate for the first time that two-dimensional Pd@Ag NSs can be used as a novel antibacterial agent for killing pathogenic bacteria upon NIR irradiation. The Pd@Ag NSs are easily prepared and exhibit an excellent photothermal effect to generate heat under the irradiation of NIR light with a low power density. While the generated heat helps to kill bacteria, NIR light can trigger the release of Ag^+, which enables persistent bactericidal activity against possible residual pathogenic virulence factors. Both Gram-positive and Gram-negative bacteria incubated with Pd@Ag NSs can be killed effectively by the synergic effect of plasmonic heating and Ag^+ release. Pd@Ag NSs are a class of promising antibacterial nanomaterials for killing antibiotic-resistant bacteria as well as the treatment of *in vivo* pathogenic bacterial biofilms or infections.

Acknowledgements

The work was financially supported by the National Natural Science Foundation of China (No. 21101131, 221420102001, 21131005), National Basic Research Foundation (973) of China (2014CB932004, 2011CB932403), Natural Science Foundation of Fujian Province (No. 2012J01056), Fundamental Research Funds for the Central Universities (2010121015), and the open project grant from State Key Laboratory of Chemo/biosensing and Chemometrics (2013009).

Notes and references

1 H. Nikaido, *Annu. Rev. Biochem.*, 2009, **78**, 119–146.
2 A. Koul, E. Arnoult, N. Lounis, J. Guillemont and K. Andries, *Nature*, 2011, **469**, 483–490.
3 B. Spellberg, R. Guidos, D. Gilbert, J. Bradley, H. W. Boucher, W. M. Scheld, J. G. Bartlett and J. Edwards Jr., *Clin. Infect. Dis.*, 2008, **46**, 155–164.

Published on 23 June 2015. Downloaded by Xiamen University on 8/17/2018 7:09:25 AM.

4 Y. Yamakoshi, N. Umezawa, A. Ryu, K. Arakane, N. Miyata, Y. Goda, T. Masumizu and T. Nagano, *J. Am. Chem. Soc.*, 2003, **125**, 12803–12809.
5 M. L. Embleton, S. P. Nair, B. D. Cookson and M. Wilson, *Microb. Drug Resist.*, 2004, **10**, 92–97.
6 L. Sun, Y. Qin, Q. Cao, B. Hu, Z. Huang, L. Ye and X. Tang, *Chem. Commun.*, 2011, **47**, 12628–12630.
7 S. Chernousova and M. Epple, *Angew. Chem., Int. Ed.*, 2013, **52**, 1636–1653.
8 N. G. Durmus, E. N. Taylor, K. M. Kummer and T. J. Webster, *Adv. Mater.*, 2013, **25**, 5706–5713.
9 Y. Zhao, Z. Chen, Y. Chen, J. Xu, J. Li and X. Jiang, *J. Am. Chem. Soc.*, 2013, **135**, 12940–12943.
10 C. Fasciani, M. J. Silvero, M. A. Anghel, G. A. Arguello, M. C. Becerra and J. C. Scaiano, *J. Am. Chem. Soc.*, 2014, **136**, 17394–17397.
11 Y. Zhao, C. Ye, W. Liu, R. Chen and X. Jiang, *Angew. Chem., Int. Ed.*, 2014, **53**, 8127–8131.
12 M. Han, X. Gao, J. Z. Su and S. Nie, *Nat. Biotechnol.*, 2001, **19**, 631–635.
13 S. Kang, M. Pinault, L. D. Pfefferle and M. Elimelech, *Langmuir*, 2007, **23**, 8670–8673.
14 X. Liu, L. Yu, F. Liu, L. Sheng, K. An, H. Chen and X. Zhao, *J. Mater. Sci.*, 2012, **47**, 6086–6094.
15 P. C. Ray, S. A. Khan, A. K. Singh, D. Senapati and Z. Fan, *Chem. Soc. Rev.*, 2012, **41**, 3193–3209.
16 H. Wang, J. Shen, G. Cao, Z. Gai, K. Hong, P. R. Debata, P. Banerjee and S. Zhou, *J. Mater. Chem. B*, 2013, **1**, 6225–6234.
17 D. Huo, J. Gao, B. Guo, Y. Ding, J. He, H. Yu, Z. Zhou and Y. Hu, *RSC Adv.*, 2013, **3**, 10632–10638.
18 E. Ju, Z. Li, M. Li, K. Dong, J. Ren and X. Qu, *Chem. Commun.*, 2013, **49**, 9048–9050.
19 M.-C. Wu, A. R. Deokar, J.-H. Liao, P.-Y. Shih and Y.-C. Ling, *ACS Nano*, 2013, **7**, 1281–1290.
20 Y.-W. Wang, Y.-Y. Fu, L.-J. Wu, J. Li, H.-H. Yang and G.-N. Chen, *J. Mater. Chem. B*, 2013, **1**, 2496–2501.
21 K. C. Black, T. S. Sileika, J. Yi, R. Zhang, J. G. Rivera and P. B. Messersmith, *Small*, 2014, **10**, 169–178.
22 M. Ramasamy, S. S. Lee, D. K. Yi and K. Kim, *J. Mater. Chem. B*, 2014, **2**, 981–988.
23 X. Huang, S. Tang, X. Mu, Y. Dai, G. Chen, Z. Zhou, F. Ruan, Z. Yang and N. Zheng, *Nat. Nanotechnol.*, 2011, **6**, 28–32.
24 S. Tang, M. Chen and N. Zheng, *Small*, 2014, **10**, 3139–3144.
25 W. Fang, S. Tang, P. Liu, X. Fang, J. Gong and N. Zheng, *Small*, 2012, **8**, 3816–3822.
26 L. Nie, M. Chen, X. Sun, P. Rong, N. Zheng and X. Chen, *Nanoscale*, 2014, **6**, 1271–1276.
27 Z. Zhao, S. Shi, Y. Huang, S. Tang and X. Chen, *ACS Appl. Mater. Interfaces*, 2014, **6**, 8878–8885.
28 Z. X. Zhao, Y. Z. Huang, S. G. Shi, S. H. Tang, D. H. Li and X. L. Chen, *Nanotechnology*, 2014, **25**, 285701.
29 X. Huang, S. Tang, B. Liu, B. Ren and N. Zheng, *Adv. Mater.*, 2011, **23**, 3420–3425.
30 S. Shi, X. Zhu, Z. Zhao, W. Fang, M. Chen, Y. Huang and X. Chen, *J. Mater. Chem. B*, 2013, **1**, 1133–1141.
31 M. Chen, S. Tang, Z. Guo, X. Wang, S. Mo, X. Huang, G. Liu and N. Zheng, *Adv. Mater.*, 2014, **26**, 8210–8216.
32 G. S. Metraux and C. A. Mirkin, *Adv. Mater.*, 2005, **17**, 412–415.
33 J. Liu and R. H. Hurt, *Environ. Sci. Technol.*, 2010, **44**, 2169–2175.
34 W. Vollmer and S. J. Seligman, *Trends Microbiol.*, 2010, **18**, 59–66.
35 Z. M. Xiu, Q. B. Zhang, H. L. Puppala, V. L. Colvin and P. J. Alvarez, *Nano Lett.*, 2012, **12**, 4271–4275.

 This journal is © The Royal Society of Chemistry 2015